

Shearing flows of frictionless spheres over bumpy planes: slip velocity

Diego Berzi · Dalila Vescovi

Received: date / Accepted: date

Abstract Boundary conditions for the slip velocity of inelastic, frictionless spheres interacting with bumpy walls are derived via discrete element method simulations of Couette granular flows. The bumpiness is created by gluing spheres identical to those flowing in a regular hexagonal array to a flat plane. Depending on the particle inelasticity and bumpiness, the characteristics of the flow range from simple shearing to plug flow. At low bumpiness - small distance between the wall-particles - the ratio of particle shear stress to pressure is a non-linear function of the slip velocity and presents a maximum. At high bumpiness, the bumpy plane behaves as a flat, frictional surface and the stress ratio saturates to a constant value for large slip velocity.

Keywords Granular flow · Boundary condition · Kinetic theory

1 Introduction

Continuum mathematical modeling of granular materials, capable of quantitatively reproducing their behaviour in a large range of flow regimes, seem now feasible. A large amount of work has been dedicated to determining appropriate constitutive relations for, e.g., the particle stress tensor.

One of the possible approaches is based on kinetic theory of dense granular gases [1,2], recently modified to take into account the role of friction [3,4], velocity correlation induced by inelasticity in collisions [5] and finite particle

D. Berzi
Politecnico di Milano, Milano 20133, Italy
Tel.: +39-02-23996262
Fax: +39-02-23996298
E-mail: diego.berzi@polimi.it

D. Vescovi
University of Twente, Enschede 7500AE, The Netherlands

stiffness [6, 7]. Conversely, considerably less efforts have been put on the analysis of boundary conditions. Given that many granular flows of interest have a thickness of a few diameters, the boundaries strongly influence the problem.

Theoretical expressions for slip velocity and fluctuation energy flux are available for rigid spheres interacting with bumpy walls [8] - where the bumpiness is due to hemispheres attached to a flat surface in a regular fashion - and flat, frictional surfaces [9, 10]. Richman [8] derived the boundary conditions for bumpy walls assuming that the particles were nearly elastic and that the ratio of the slip velocity to the square root of the granular temperature - mean square of the particle velocity fluctuations - was less than unity. Jenkins et al. [11] analysed the case of nearly elastic spheres flowing over a bumpy wall in which the bumpiness was due to hemicylinders perpendicular to the flow direction attached to the wall, removing any limits on the value of the slip velocity. Unfortunately, that work is still unpublished, but those boundary conditions have been reported in Ref. [12].

Here, we extend our previous work [13] on discrete element simulations of steady flows of identical, inelastic, frictionless spheres between parallel, bumpy planes in absence of gravity. The particle motion is driven by one of the plane moving at constant velocity (Couette granular flow). The bumpiness is due to spheres, identical to those flowing, attached to the planes in a regular hexagonal array. By changing the particle inelasticity and the distance between the wall-particles, we infer expressions for the slip velocity that phenomenologically extend the analysis of Richman and Jenkins et al. for the case of low bumpiness. At high bumpiness, we show that the bumpy wall made of frictionless spheres behaves as a frictional, flat surface.

2 Simulations and results

We simulate the steady shearing flow of monodispersed, frictionless spheres (of density ρ_p and diameter d) between two parallel, bumpy planes in absence of gravity through the Discrete Element Method [13]. The particles are characterized by a coefficient of collisional restitution e (negative ratio of post- to pre-collisional normal relative velocity between two colliding spheres) and by the stiffness k of the linear spring in the spring-dashpot model used to represent the particle interactions in the DEM simulations. The flow configuration is depicted in Fig. 1. The coordinates along the flow, shearing and vorticity directions are x , y and z , respectively. We use periodic boundary conditions along x and z and we move the upper plane at a constant velocity V , while the other is at rest. The walls are made bumpy by gluing spheres, identical to the flowing particles, in a regular, hexagonal fashion. In all simulations, the distance H between the edges of the particles glued at the moving and resting walls has been kept constant and equal to 18 diameters. The bumpiness of the walls can be measured by the distance l between the edges of adjacent particles glued at them (Fig. 1). Equivalently, we can use the angle ψ , defined as $\sin \psi = (d+l)/(2d)$ [8]. The minimum bumpiness is when $l = 0$, i.e., $\psi = 5\pi/30$,

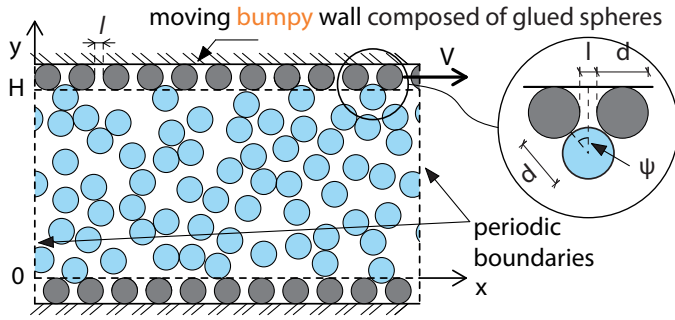


Fig. 1 Sketch of the flow configuration with the frame of reference.

corresponding to a minimum effective penetration angle, in the hexagonally packed wall-spheres layer, of about $\pi/5$. Conversely, when $\psi \geq \pi/3$, the flowing spheres can fully penetrate in the gaps between the particles glued at the walls.

We set the particle density and diameter and the velocity of the moving wall equal to unity, so that all the variables in the problem are dimensionless. We perform the simulations with a fixed $k = 2 \cdot 10^5$ and we change the coefficient of restitution e in the range 0.2 to 0.98, the bumpiness ψ in the range $5\pi/30$ to $12\pi/30$ and the spatial-averaged volume fraction in the domain $\bar{\nu}$ in the range 0.2 to 0.44. We uniformly divide the domain along the y -direction in slices of thickness less than one diameter and we perform space-time averaging in every slice to obtain profiles of particle x -velocity, u , solid volume fraction, ν , and granular temperature, T . We indicate with u_w , ν_w and T_w the values of particle x -velocity, solid volume fraction and granular temperature at a distance of half a diameter from the top of the particles glued at the resting wall. This is the location at which the boundary conditions for the shearing flows of spheres over bumpy planes derived by Richman [8] apply and u_w is the slip velocity. We also measure the particle pressure p and shear stress s (both constant in the flow in absence of gravity due to momentum balance).

In a previous work [13], we showed that, at a given bumpiness, there is a minimum value of the coefficient of restitution for the simulation to reach a steady state. Lower values of the coefficient of restitution imply a collapse of the particles in the core and lack of collisions with the bumpy walls: energy cannot be therefore supplied to the flowing particles from the boundaries and the kinetic energy of the particles decays following the Haff's law [14] (Homogeneous Cooling State, HCS). Here, we have investigated a larger portion of the parameter space and we are able to present a more complete picture of the flow regimes encompassed by granular Couette flows between bumpy planes. The value of the slip velocity is determined by the combination of coefficient of restitution and bumpiness, at a given value of $\bar{\nu}$. Figure 2 represents the contour plot of u_w in terms of e and ψ when $\bar{\nu} = 0.4$. For symmetry reasons, the value of the slip velocity lies in the range between 0 and 0.5. Zero slip velocity implies a linear velocity profile and uniform distributions of solid volume frac-

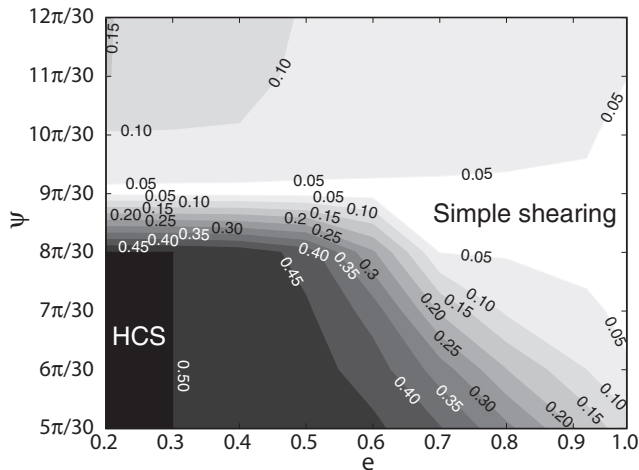


Fig. 2 Contour plot of slip velocity when $\bar{\nu} = 0.4$. White and black areas represent the regions of existence of simple shearing and homogeneous cooling state, respectively.

tion and granular temperature, i.e., simple shearing. Slip velocity equal to 0.5 implies the existence of a plug flow in the core, the lack of contacts between the walls and the flowing particles and the already mentioned HCS. In between these two extremes, there are a number of intermediate states. Figure 2 indicates that granular Couette flows reach HCS for rather low values of the coefficient of restitution and low bumpiness. The condition of simple shearing is instead possible for every value of e in a range of bumpiness which narrows down as the coefficient of restitution decreases.

We now analyse separately the two extreme cases of low ($\psi \leq 8\pi/30$) and high bumpiness ($\psi \geq 10\pi/30$) for the simulations which reach steady state. It is worth recalling that when ψ exceeds $\pi/3$ the flowing particles can actually fall and be trapped in the gaps between the wall's spheres. The case $\psi = 9\pi/30$ is intermediate between these two extremes.

2.1 Low bumpiness

As already mentioned, Richman's [8] analysis provides an expression for the slip velocity of nearly elastic spheres flowing over a wall at which hemispheres are glued in a regular, hexagonal array:

$$\frac{u_w}{T_w^{1/2}} = \left(\frac{\pi}{2}\right)^{1/2} f \frac{s}{p}, \quad (1)$$

where f is a rather complicated function of the bumpiness and the solid volume fraction ν_w . Equation (1) is valid for nearly elastic spheres and small (less than unity) values of $u_w/T_w^{1/2}$. A consequence of the latter assumption is the linear relation between the stress ratio s/p and the slip velocity.

Jenkins et al. [11] analysed the case of nearly elastic spheres flowing over a wall in which hemicylinders perpendicular to the flow direction are glued. By not assuming small values of $u_w/T_w^{1/2}$, they obtained a non-linear relation between the stress ratio and the slip velocity. Their expression, as reported in Ref. [12], reads

$$\frac{u_w}{T_w^{1/2}} = \left(\frac{\pi}{2}\right)^{1/2} \frac{1}{\psi \csc \psi - \cos \psi} \frac{s}{p} C, \quad (2)$$

where $C = 1 + \left(\psi u_w/T_w^{1/2}\right)^2 / 3$. Equation (2) is a simple expression that can be easily employed in continuum mathematical models of granular flows. Here, we want to check if it holds also for the case of inelastic spheres impacting like-spheres glued at the walls, only by modifying the dependence of C on the scaled slip velocity $\psi u_w/T_w^{1/2}$. Inverting Eq. (2), and using the numerical values of u_w , T_w , s and p from the simulations for different ψ and $\bar{\nu}$, we can obtain C as function of $\psi u_w/T_w^{1/2}$. Actually, we did not employ the value of T_w obtained from the simulations, because it is now clear that the granular temperature is very sensitive to the averaging method, especially close to the walls where the velocity gradients are important [15,16]. In our previous work [13], we have shown that the relation between particle pressure, granular temperature and solid volume fraction, i.e., the equation of state, away from the walls is well predicted by kinetic theory [2],

$$p = [1 + 2(1 + e)\nu^2 g_0] T, \quad (3)$$

if the radial distribution function at contact g_0 suggested by Vescovi et al. [13] is employed:

$$g_0 = f \frac{2 - \nu}{2(1 - \nu)^3} + (1 - f) \frac{2}{\nu_s - \nu}, \quad (4)$$

where

$$f = \begin{cases} 1 & \text{if } \nu < 0.4, \\ \frac{\nu^2 - 0.8\nu + \nu_s(0.8 - \nu_s)}{0.8\nu_s - 0.16 - \nu_s^2} & \text{otherwise.} \end{cases} \quad (5)$$

In Equation (4), ν_s is the shear rigidity volume fraction, defined as the largest volume fraction at which a randomly collisional granular material can be sheared without force chains spanning the entire domain. For frictionless particles, ν_s is equal to 0.636.

To avoid the uncertainties in the granular temperature at the wall, we therefore obtain T_w by inverting Eq. (3) and using the more reliable numerical values of solid volume fraction ν_w and pressure p . We nonetheless emphasize that the usage of the measured values of the granular temperature would not qualitatively change the results. Furthermore, we point out that in this work we have chosen to assume a unique equation of state, valid anywhere in the domain. In so doing, we indeed disregard the influence of the walls on the radial distribution function, which can be affected by layering effects. We are aware that this approach does not completely represent the physics of the problem

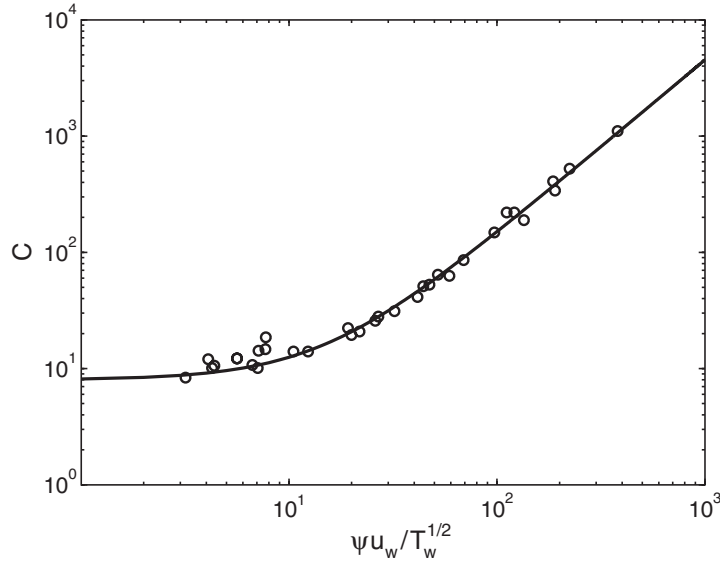


Fig. 3 Coefficient C as a function of $\psi u_w / T_w^{1/2}$ from the present simulations (circles) when $5\pi/30 \leq \psi \leq 8\pi/30$ (all values of $\bar{\nu}$ and e). The solid line represents Eq. (6).

at the walls, but it has the big advantage of providing boundary conditions that can be consistently applied to models in which the equation of state is independent of spatial coordinates. Figure 3 shows a nice collapse of the values of C as a function of $\psi u_w / T_w^{1/2}$, irrespective of the value of the coefficient of restitution. A good fitting is obtained for

$$C = 8 + \frac{1}{7} \left(\psi \frac{u_w}{T_w^{1/2}} \right)^{3/2}. \quad (6)$$

Defining the scaled stress ratio as

$$R = \left(\frac{\pi}{2} \right)^{1/2} \frac{\psi}{\psi \csc \psi - \cos \psi} \frac{s}{p}, \quad (7)$$

and, using Eq. (6) in Eq. (2) and re-arranging, we obtain

$$R = \psi \frac{u_w}{T_w^{1/2}} \left[8 + \frac{1}{7} \left(\psi \frac{u_w}{T_w^{1/2}} \right)^{3/2} \right]^{-1}. \quad (8)$$

When the numerical values of the scaled stress ratio are plotted against the numerical values of the scaled slip velocity (Fig. 4), it is even more evident the collapse of the data for different values of bumpiness, coefficient of restitution and average solid volume fraction and the good agreement of Eq. (8) with the simulations. The non-linearity between the stress ratio and the slip velocity - the scaled slip velocity is as large as 400 in our simulations - results in the presence of a maximum $R \approx 1$ for $\psi u_w / T_w^{1/2} \approx 25$.

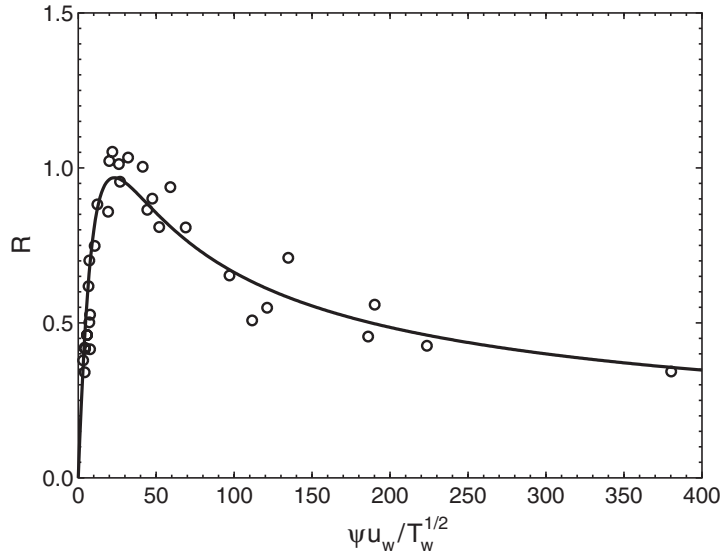


Fig. 4 Scaled stress ratio as a function of scaled slip velocity from the present simulations (circles) when $5\pi/30 \leq \psi \leq 8\pi/30$ (all values of $\bar{\nu}$ and e). The solid line represents Eq. (8).

2.2 High bumpiness

The case ψ larger than $10\pi/30$ is completely different. The stress ratio s/p shows no significant influence of bumpiness or coefficient of restitution when plotted versus $u_w/T_w^{1/2}$ (Fig. 5). The stress ratio initially increases linearly with the slip velocity - seemingly having a non-zero value at $u_w = 0$ (yielding) - and saturates to a constant value of approximately 0.55 at large values of $u_w/T_w^{1/2}$. This behaviour resembles closely what theoretically derived with spheres flowing over a flat, frictional surface [9]. In this sense, the limit value 0.55 represents an equivalent friction coefficient for very bumpy walls. It is worth emphasizing that this frictional behaviour has been obtained in absence of interparticle friction. We propose the following simple fitting of the data:

$$\frac{s}{p} = \min \left(0.1 + 0.01 \frac{u_w}{T_w^{1/2}}; 0.55 \right). \quad (9)$$

The presence of a yielding value of the stress ratio, and the saturation to a constant value at large slip velocities, is in accordance with experiments on incline flows of glass spheres over rough surfaces [17]. Those experiments, indeed, revealed that steady incline flows existed only in a range of angles of inclination: for angles of inclination less than a minimum (corresponding to the yielding value of Fig. 5), flows would decelerate and come to rest; for angles of inclination larger than a maximum (corresponding to the saturation value of Fig. 5), flows would accelerate indefinitely. The value 0.1 for the yielding

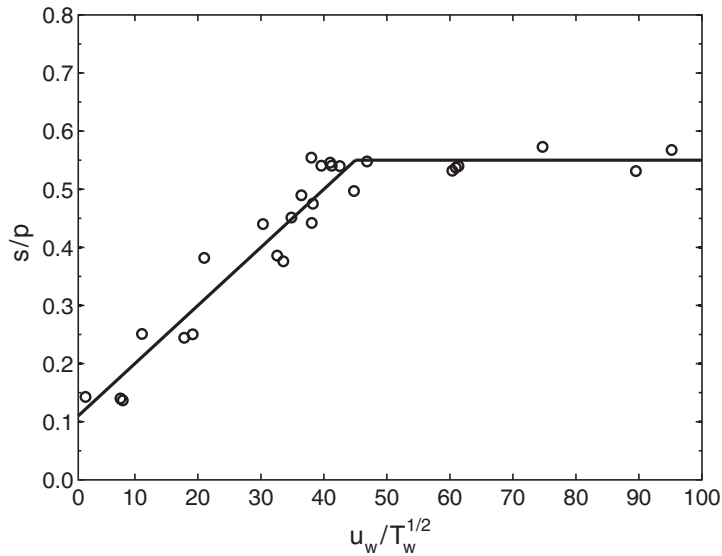


Fig. 5 Stress ratio as a function of $u_w/T_w^{1/2}$ from the present simulations (circles) when $10\pi/30 \leq \psi \leq 12\pi/30$ (all values of e). The solid line represents Eq. (9).

the stress ratio is very close to that of frictionless spheres obtained in simple shearing [4].

3 Conclusions

We have numerically simulated, through the discrete element method, the steady Couette flow of frictionless, inelastic spheres. We made the walls bumpy by attaching to them spheres identical to those flowing. We have changed the number of particles in the flow, the particle inelasticity and the distance between the hexagonally placed wall-particles and measured the slip velocity as a function of the local granular temperature, particle pressure and shear stress. We have shown how the combination of bumpiness and particle inelasticity causes the flow to have the characteristics of simple shearing, plug flow or being intermediate between those two extremes. At low bumpiness, we have obtained values of the slip velocity, scaled with the square root of the granular temperature, much greater than one (as large as 400). As a consequence the stress ratio is a non-linear function of the scaled slip velocity and presents a maximum. At large bumpiness, the scaled slip velocity is only a function of the stress ratio - independent of bumpiness and particle inelasticity. The stress ratio initially increases linearly with the scaled slip velocity and then saturates to a constant value. This behaviour is typical of flat, frictional surface. The fact that an effective macroscopic frictional behaviour has been obtained by adding frictionless bumps to a plane is reminding of microscopic models of contact friction.

Acknowledgements The authors would like to thank Prof. James T. Jenkins for sharing his unpublished manuscript and for several fruitful discussions of the problem.

References

1. J.T. Jenkins and S.B. Savage, A theory for the rapid flow of identical, smooth, nearly elastic, spherical particles, *J. Fluid Mech.*, 130, 187-202 (1983)
2. V. Garzo and J.W. Dufty, Dense fluid transport for inelastic hard spheres, *Phys. Rev. E*, 59, 5895-5911 (1999)
3. J.T. Jenkins and C. Zhang, Kinetic theory for identical, frictional, nearly elastic spheres, *Phys. Fluids*, 14, 1228-1235 (2002)
4. D. Berzi and D. Vescovi, Different singularities in the functions of extended kinetic theory at the origin of the yield stress in granular flows, *Phys. Fluids*, 27, 013302 (2015)
5. J.T. Jenkins, Dense inclined flows of inelastic spheres, *Granul. Matt.*, 10, 47-52 (2007)
6. D. Berzi, D. Vescovi and C.G. di Prisco, Constitutive relations for steady, dense granular flows, *Phys. Rev. E*, 84, 031301 (2011)
7. D. Berzi and J.T. Jenkins, Steady shearing flows of deformable, inelastic spheres, *Soft Matt.*, 11, 4799-4808 (2015)
8. M.W. Richman, Boundary conditions based upon a modified Maxwellian velocity distribution for flows of identical, smooth, nearly elastic spheres, *Acta Mech.*, 75, 227-240 (1988)
9. J.T. Jenkins, Boundary Conditions for Rapid Granular Flow: Flat, Frictional Walls, *J. Appl. Mech.*, 59, 120-127 (1992)
10. J.T. Jenkins and M. Louge, On the flux of fluctuation energy in a collisional grain flow at a flat, frictional wall, *Phys. Fluids*, 9, 2835-2840 (1997)
11. J.T. Jenkins, S. Myagchilov and H. Xu, Nonlinear Boundary Conditions for Collisional Grain Flows at Bumpy, Frictional Walls (unpublished)
12. H. Xu, M. Louge and A. Reeves, Solutions of the kinetic theory for bounded collisional granular flows, *Cont. Mech. Thermodyn.*, 15, 321-349 (2003)
13. D. Vescovi, D. Berzi, P. Richard and N. Brodu, Plane shear flows of frictionless spheres: Kinetic theory and 3D soft-sphere discrete element method simulations, *Phys. Fluids*, 26, 053305 (2014)
14. P. Haff, Grain flow as a fluid-mechanical phenomenon, *J. Fluid Mech.*, 134, 401-430 (1983)
15. T. Weinhart, R. Hartkamp, A.R. Thornton and S. Luding, Coarse-grained local and objective continuum description of three-dimensional granular flows down an inclined surface, *Phys. Fluids*, 25, 070605 (2013)
16. R. Artoni and P. Richard, Average balance equations, scale dependence, and energy cascade for granular materials, *Phys. Rev. E*, 91, 032202 (2015)
17. O. Pouliquen, Scaling laws in granular flows down rough inclined planes, *Phys. Fluids*, 11, 542-548 (1999)